

## A BRIEF OBSERVATION OF THE FORMATION OF COHERENT STRUCTURES AND TURBULENCE OVER A RAIN FOREST AREA IN CENTRAL AMAZONIA: THE ATTO-CLAIRE / IOP – 1/2012 EXPERIMENT

Newton S. Lima<sup>1</sup>, Júlio Tóta<sup>2</sup>, Maurício J.A. Bolzan<sup>3</sup>, Alan S. Ferreira<sup>1</sup> and Matheus R. Pietzsch<sup>1</sup>

**ABSTRACT.** This work used micrometeorological measurements of temperature and wind in order to characterize the turbulence due to wind in a *terra firme* forest in Central Amazônia as part of the ATTO-CLAIRE / IOP-1 (2012) (*Amazon Tall Tower Observatory – Cooperative LBA Airborne Regional Experiment / Intensive Observation Period – 2012 / LBA – Large Scale Biosphere-Atmosphere Experiment in the Amazônia*). This research was conducted at the Uatumã ATTO Sustainable Development Reserve in the State of Amazonas, Brazil, from February to September, 2012, and used data from February 26 to September 07, 2012, dates that partially encompass the wet and dry seasons, respectively. The ATTO site has 5 towers: one that is 320 m, and four that are 80 m in height, and this research was conducted on an 80 m triangular tower. A total of ten 3D and 2D ultrasonic anemometers were installed on the tower, and the importance of these instruments used for flux measurements is also evident when taking into account the fact that the dissemination and diffusion of seeds and chemical composts in the forest happens through the action of turbulent fluxes. In order to understand the wind profile, the inflection point of the wind velocity, and coherent structures (ECs) and local turbulence, box-plot diagrams, quadrant analyses, wavelet potential spectrum, and energy potential analyses were conducted. The turbulence characterized at the ATTO had a roll or ramp structure during the study period, which represents favorable conditions for the maintenance of the forest during the wet and dry seasons in the Central Amazônia.

**Keywords:** inflection point, ramp, wavelet, turbulence.

**RESUMO.** Este trabalho faz uso de medidas micrometeorológicas de temperatura e vento, com finalidade de caracterizar a turbulência aerotransportada em uma floresta de *terra firme* na Amazônia Central, realizadas no experimento ATTO-CLAIRE / IOP-1 (2012) (*Amazon Tall Tower Observatory – Cooperative LBA Airborne Regional Experiment / Intensive Observation Period – 2012 / LBA – Large Scale Biosphere-Atmosphere Experiment in Amazônia*), no sítio do ATTO, na Reserva de Desenvolvimento Sustentável do Uatumã – AM (Brasil) nos meses de fevereiro a setembro de 2012, com dados analisados a partir do dia 26 de fevereiro de 2012 até o dia 7 de setembro de 2012, entre as estações úmida e seca na Amazônia Central, no complexo de torres altas composto por 5 (cinco) torres; 1 (uma) de 320 m e 4 (quatro) de 80 m. Este trabalho foi realizado na torre triangular (80 m). Foram instalados 10 (dez) anemômetros ultrassônicos de 3D e 2D. Equipamentos necessários em método de fluxos, visto que, a disseminação e difusão de sementes e compostos químicos da floresta, faz-se também por fluxos turbulentos. Para compreensão do perfil de vento, ponto de inflexão do perfil da velocidade do vento, estruturas coerentes e a turbulência local, para tal desenvolveu-se a partir dos dados processados, diagrama de caixa (*box-plot*), análise de quadrantes, espectro de potência em ondeletas, espectro de energia. A turbulência caracterizada no ATTO, foi de estruturas do tipo “rolo” ou rampa, para o período estudado, condições favoráveis para manutenção da floresta em período úmido-seco na Amazônia Central.

**Palavras-chave:** ponto de inflexão, rampa, ondeleta, turbulência.

<sup>1</sup>Centro Universitário Luterano de Manaus (CEULM/ULBRA), Av. Carlos Drummond de Andrade, 1460, Japiim II, 69077-730 Manaus, AM, Brazil. Phone: +55(92) 3616-9800 – E-mails: newtonulbra@gmail.com; alans\_ferreira@hotmail.com; ulbramada@yahoo.com.br

<sup>2</sup>Universidade Federal do Oeste do Pará, Vera Paz Street, s/n (Unidade Tapajós), Bairro Salé, 68040-255 Santarém, PA, Brazil – E-mail: totaju@gmail.com

<sup>3</sup>Universidade Federal de Goiás, Rua Riachuelo, 1530, Sector Samuel Graham, 75804-020 Jataí, GO, Brazil – E-mail: mauricio.bolzam@gmail.com

## INTRODUCTION

The study of the dynamics of the atmospheric flow in a dry forest area of Central Amazônia (Brazil) highlights the importance of the vertical profile of the average wind velocity in the formation of coherent structures and the instability of the inflection point over the forest crown cover during daytime, night-time, and transition phases. To understand the interaction between forest and atmosphere, it was necessary to understand the turbulent changes in the atmospheric boundary layer (ABL). The ABL evolves continuously as a response to surface heating or cooling. It is characterised by different states that can be accurately described by transition phases (day-night and/or vice versa) (Kaimal & Finnigan, 1994).

In a literature review by Dennis (2015), the author studied turbulence and the manners in which researchers approach the subject in an attempt to deconstruct the complex and unorganized field of turbulent flux into a set of organized movements that, to a certain degree, are generally referred to as “coherent structures”, thus indicating their singularity.

Raupach et al. (1996) suggested that in order to study the characteristics of active turbulence and coherent movements, above the canopy of a *terra firme* forest, it would be necessary to model them in a mixed flat layer, due to the instability associated with the strong inflection characteristic in the average wind velocity profile. Additionally, Raupach (1992), emphasizes that an analytical treatment must be conducted with respect to drag on rough surfaces in order to develop simple predictive capabilities that have practical applications and make sense of atmospheric data in order to formalize the intrinsic character of the analysis.

The chaotic nature of turbulence in the atmospheric boundary layer, in the interior and above the forest canopy, was investigated by Campanharo et al. (2005), using a temporal series that included components that were described individually in a *terra firme* forest in the Amazon. In their study the objective was to identify a low-dimension chaotic attractor, which was not the goal of the present study. However, Dias Jr. et al. (2013) discuss the vertical variability of coherent structures in the convective boundary layer in the Amazon, indicating that ECs present a reduction in their duration as they approach the forest canopy due to the coalescence of turbulent vortices, thus emphasizing the importance of the study of ECs.

Lima et al. (2013) presented a brief introduction of the aerodynamic characteristics of turbulence above and within the forest canopy in relation to an EC in a *terra firme* forest in the Central

Amazônia, thus contributing in loco measurements to the field of observational studies.

In the forest of the Uatumã River (AM), the registered floristic composition shows 741 individuals (abundance) per hectare, including vines, lianas, and palms, and this result is within the average for the Amazon region according to Rankin-de-Mérona et al. (1992: 618 individuals), Valencia et al. (1994: 693), and Tello (1995: 747), *apud* Amaral et al. (2000). Andreae et al. (2015) highlight the importance of biodiversity and the ecosystems of the ATTO when they emphasize that it is essential to establish long-term measurement plots that can provide a baseline of actual climate, biogeochemical, and atmospheric conditions that could be used in the coming decades in order to monitor changes in the Amazon region with respect to expected increases in human perturbation the near future, which represents a large source of pre-occupation in the northern region of South America. All the data collected from these natural processes demonstrate that aerodynamic transport through turbulence is an important and essential contributor to the maintenance of life in the forest.

## MATERIAL AND METHOD

### Study Area

The Amazon Tall Tower Observatory (ATTO) was the first large environmental observatory in South America, with a 320-metre Tower (Fig. 1) and four peripheral 80-metre towers. It is located in the Sustainable Development Reserve of Uatumã (SDR), São Sebastião do Uatumã, AM, Brazil (2°08'32.42"S; 59°0'3.50"W; Altitude: 131 m) as shown in Figure 2A. The data of this experiment are shown with frequencies of 1 Hz, 4 Hz, and 10 Hz collected from 26th February to 7th September 2012. In the intensive observation period – I (IOP-1/2012), we used three 3D ultrasonic anemometers (Solent, Gill Instruments Ltd., UK), three 2D WindSonic ultrasonic anemometers (Gill Instruments Ltd., UK) and four 2D-Wind Speed & Direction Sensor ultrasonic anemometers (Gill Instruments Ltd., UK) (Table 1). The tower of the present study has the following characteristics: 80 metres high and triangular cross-section area of 0.156 m<sup>2</sup> (Fig. 2B). The leaf area index (LAI) in this area is around 5 to 6 m<sup>2</sup>.m<sup>-2</sup> (Oliveira, 2008). The equipment was positioned at the following sampling heights: 78 m; 41 and 30 m for the Wind Master; 57 m; 70 and 62 m for the Met Pack; 23 m; 36 m; and 45 and 50 m for the WindSonic. There was northeast wind predominance and the average vegetation height ranged from 40 to 45 metres, approximately.



**Figure 1** – Amazon Tall Tower Observatory (ATTO); height: 320 m. Source: INPA – MAX PLANCK (2014).

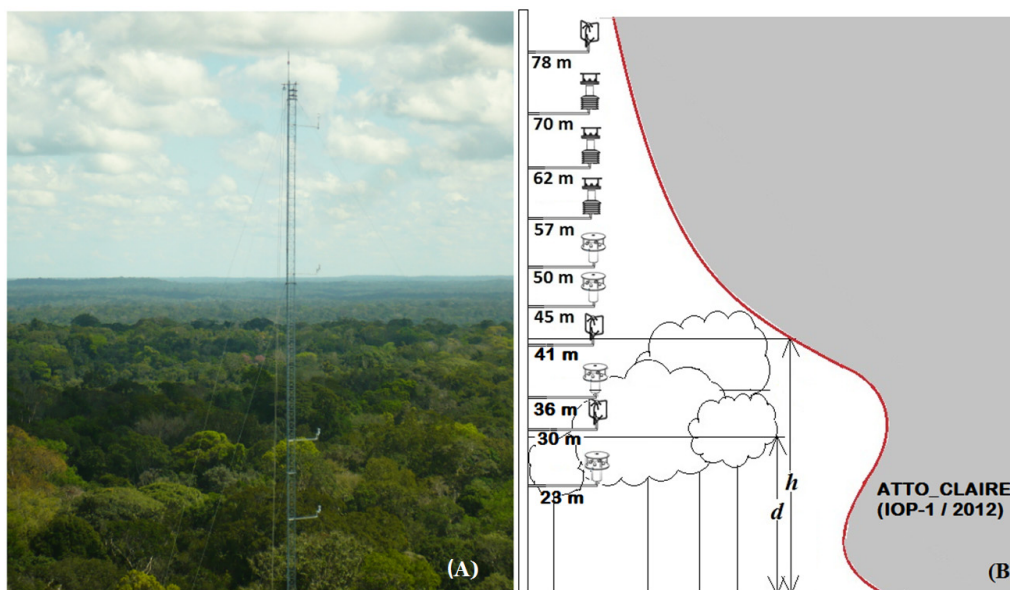


**Figure 2** – (A): ATTO-CLAIRE (IOP-1/2012) experiment; tower height: 80 m; (B): outline of the experiment ( $2^{\circ}8'32.42''S$ ;  $59^{\circ}0'3.50''W$ , Altitude: 131 m). Note: not in scale. Source: INPA-UEA-LBA (2012).

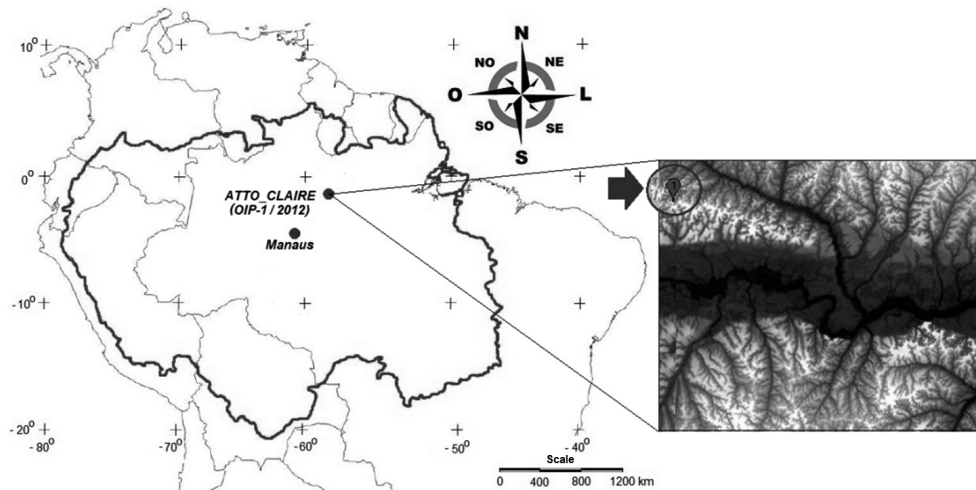


**Figure 3** – ATTO-CLAIRE (IOP-1/2012) experimental site plateau located in the Sustainable Development Reserve of Uatumbã, in the Amazon basin, AM (surrounded). The darkest colour in the grey figure (lower elevations) illustrates the rivers, the Uatumbã River being the widest, and the lightest colour illustrates the highest elevations. (Source: INPA – MAX PLANCK; SRTM – USGS-NASA, 2012).

**Table 1** – Instrumentation of turbulent fluxes measurement at ATTO-CLAIRE (INPA – MAX PLANCK) (IOP-1) during the observation period (February-September 2012). The wind velocity components were: ( $u, v, w$ )  $\text{m}\cdot\text{s}^{-1}$ ; the sonic speed was ( $C$ )  $\text{m}\cdot\text{s}^{-1}$ ; the sonic, virtual, and dew point temperatures were ( $T, Tv$  and  $Td$ )  $^{\circ}\text{C} \pm 0.15^{\circ}\text{C}$ ; the direction of the wind was ( $|DirV|$ )  $0-259^{\circ} \pm 3^{\circ}$  ( $12 \text{ m}\cdot\text{s}^{-1}$ ); average velocity module ( $|v|$ )  $\text{m}\cdot\text{s}^{-1}$ ; barometric pressure ( $P$ ) hectopascal – hPa  $\pm 0.5 \text{ hPa}$ ; relative humidity (RH)  $\% \text{ RH} \pm 0.8\%$  ( $23^{\circ}\text{C}$ ); battery charge ( $BAT$ )  $\text{V} = \text{volts}$ . (Source: INPA – MAX PLANCK, 2012).

Tower (80 m)	Height	Access Code	Frequency	Ultrasonic Anemometer	Reading
Turbulent fluxes	78	USB0	10	3D <sup>1</sup>	$u, v, w, C, Tv$
	41	USB1	10	3D <sup>1</sup>	$u, v, w, C, Tv$
	30	USB2	10	3D <sup>1</sup>	$u, v, w, C, Tv$
	37	USB3	1	2D <sup>2</sup>	$DirV,  v , P, RH, T, Td, BAT$
ATTO-CLAIRE (IOP-1)	70	USB4	1	2D <sup>2</sup>	$DirV,  v , P, RH, T, Td, BAT,$
	62	USB5	1	2D <sup>2</sup>	$DirV,  v , P, RH, T, Td, BAT$
	23	USB6	4	2D <sup>3</sup>	$DirV,  v ,$
	36	USB7	4	2D <sup>3</sup>	$DirV,  v ,$
	45	USB8	4	2D <sup>3</sup>	$DirV,  v ,$
	50	USB9	4	2D <sup>3</sup>	$DirV,  v ,$

<sup>1</sup> Turbulent Fluxes Tower (IOP-1) WindMaster, Gill Instruments Ltd., UK.

<sup>2</sup> Turbulent Fluxes Tower (IOP-1) MetPak, Gill Instruments Ltd., UK.

<sup>3</sup> Turbulent Fluxes Tower (IOP-1) WindSonic, Gill Instruments Ltd., UK.

## METHODOLOGY

### Statistical Method

The components of the wind  $u$  and  $v$  were determined by the definition of average wind velocity ( $U$ ) in the direction of average horizontal flux, but without applying the correlation of the wind vertical inclination and keeping the wind component  $w$  unchanged. One of the resources used was digital processing for 600 seconds, followed by the method proposed by Lloyd et al. (1984) and Baldocchi & Meyers (1988) for separating tendencies and fluctuations ( $u$ ,  $v$ , and  $w$ ). Fluctuations can be directly compared using statistics of second- and superior-order variables. Often, basic statistic is the standard for describing turbulence at each level of observation. The vertical movement of air over the tops of the trees is shown through averages and variances to identify how the turbulence is structured in any position. Also, the covariance indicates that the movement of the wind is associated with the horizontal *momentum* transport, asymmetries (skewness) and kurtosis, thus showing that this variance of air movement is characterised by fast movement, intermittency, and descending vortices.

The raw data of 10 Hz, 4 Hz, and 1 Hz were submitted to calculation of averages of the three wind components ( $u$ ,  $v$ , and  $w$ ), as well as the variance, covariance, asymmetries (*skewnesses*), and kurtosis, using the rate  $Z/h = 2.08$  in the rough sub-layer of the forest in ATTO. The data were normalized to infer parameters such as: the average wind with height of treetops ( $u/u(h)$ ); *momentum* flux, with the ( $u_*$ ) friction wind velocity ( $\overline{u'v'}/(u_*^2)$ ), which at the top of the tower is equivalent to ( $u_*$ ) =  $(-\overline{u'v_{top}})^{1/2}$ ; for the height of the  $h = 80$ -metre tower, the standard deviations,

$$\sigma_u = (\overline{u'^2})^{1/2}/u_* \quad \text{and} \quad \sigma_w = (\overline{w'^2})^{1/2}/u_*;$$

the correlation coefficient between  $u$  and  $w$ ,  $-r + uw = -\overline{u'w'}/(\sigma_u\sigma_w)$ ; the asymmetries (skewnesses) of  $u$  and  $w$ ,  $Sk_u$  and  $Sk_w$  (e.g.,  $\overline{w'^3}/\sigma_w^3$ ); and finally, the kurtosis of  $u$  and  $w$ , (e.g.,  $\overline{w'^4}/\sigma_w^4$ ), Kaimal & Finnigan (1994), Bolzan (2000), Kruijt et al. (2000).

The calculations were used to determine the profiles of the vertical component of the wind, as well as for creating a box-plot diagram to show the variation between averages and medians at different heights, indicating dispersion, asymmetry and correlation between the vertical component of the wind and the temperature inside and over the vegetation canopy.

### Covariance Method

The covariance method allowed to directly compare the fluctuation with statistics of second- and superior-order variables.

Basic statistical analysis was used as the standard for describing turbulence at each level of observation. The vertical movement of air over the treetops is shown through averages and variances to identify how the turbulence is structured in any position.

We selected the variables of the atmosphere, including its turbulent characteristic, in order to carry out the measurements. The covariance method of direct measurement with application of empirical constants of wind components ( $w$ ) and temperature ( $T$ ) was used according to Foken's method (2008). Through statistical analysis, we determined: averages; fluctuations; standard deviation; correlation; drag coefficient, for subsequent construction of quadrant analysis graphs with linear regression; global wavelet spectrum; and energy spectrum.

The covariance of the vertical component of the wind velocity ( $w$ ) and a horizontal component of the wind, or scalar ( $x$ ), and temperature ( $T$ ) could be determined by Eq. (1).

$$\begin{aligned} \overline{w'x'} &= \frac{1}{N-1} \sum_{k=0}^{N-1} [(w_k - \overline{w})(x_k - \overline{x})] \\ &= \frac{1}{N-1} \left[ \sum_{k=0}^{N-1} w_k x_k - \frac{1}{N} \left( \sum_{k=0}^{N-1} w_k \sum_{k=0}^{N-1} x_k \right) \right] \end{aligned} \quad (1)$$

The high frequency measures were sampled at 10 Hz, 4 Hz, and 1 Hz. The instrument used was an ultrasonic anemometer, since this equipment also provides the sonic temperature (very close to virtual temperature). The flux calculated in the present study with this temperature is the sensible heat flux (Eq. 2) (Foken, 2008).

$$\frac{Q_{HB}}{\rho c_p} = \overline{w'T'_v} \quad (2)$$

in which  $Q_{HB}$  is the sensible heat flux in  $W m^{-2}$ ; and  $T_v$  is the virtual temperature in Kelvin (K) (Foken, 2008).

### Wavelet Transform

Fourier transform (FT) is a useful tool for studying the power spectrum (variance) of a stationary time series, because it provides the distribution of spectral density that identifies the "energies" associated with the frequencies and their relative contributions to the time series.

However, it does not provide information regarding its temporal location. According to Gasquet & Witomski (1990), the FT consists only of a "global" transform. Therefore, for a signal  $x(t)$ , the FT is a natural "stationary wavelet transform" defined by:

$$F(\omega) = \int_{-\infty}^{\infty} f(t)e^{-i\omega t} dt \quad (3)$$

in which  $f(t)$  is the signal to be analysed.

Therefore, the problem of FT is the inability to analyse non-stationary signals. This difficulty was observed by Gabor, who in 1946 added a “local frequency” parameter (local in time), so that the local FT, applied through a window, would operate through a signal that was approximately stationary in a given interval, what later became known as Windowed Fourier Transform (WFT). However, Gabor’s WFT method had an obstacle, i.e., the window was fixed and restricted the applicability of the method to previously chosen scales. The solution of the problem was a revolutionary innovation, i.e., the inclusion of a “variable” window which, like an accordion, could expand or compress depending on the scale of analysis (Gasquet & Witomski, 1990). This inclusion was accomplished by Morlet in the 1980s and became known as “wavelet transform” (WT) (Farge, 1992). Meyer (1990) demonstrated the orthogonality conditions of this new mathematical operator, providing safe conditions for the application of the new technique.

The term “wavelet” refers to a set of functions in the shape of small waves generated by expansions,  $\Psi(t) \rightarrow \Psi(2t)$ , and propagation,  $\Psi(t) \rightarrow \Psi(t+1)$ , of a generating simple function,  $\Psi(t)$ , i.e., mother wavelet. It should be quadratically integrable within a real time or space  $[L^2(\mathcal{R})]$ , that is, it should have finite energy. The fact that its average energy is zero constitutes the *admissibility condition* of the function. Mathematically, the wavelet function in scale  $a$  and position  $b$  is expressed by:

$$\Psi_{a,b}(t) = a^{-1/2} \Psi\left(\frac{t-b}{a}\right) \quad (4)$$

in which  $a$  and  $b$  are real and  $a > 0$ . It should be noted that the Eqs. (4) and (5) include the normalization term  $a^{-1/2}$ . Wavelet transform is defined by:

$$(W_{\psi}f)(a,b) = \frac{1}{|a|^{1/2}} \int f(t) \psi\left(\frac{t-b}{a}\right) dt \quad (5)$$

in which the temporal function  $f(t)$  is the series of data to be analysed.

The Eqs. (4) and (5) are similar and the only difference is the nucleus (kernel) of the equations, i.e., the nucleus in the FT is given by an exponential function and in the WT by a wavelet function.

There is the possibility of using different types of wavelet functions for WT depending only on the need. This way, these different types of wavelet functions can be classified into two large groups, namely: *continuous wavelets* and *discrete wavelets*. Among the best-known discrete wavelets are Haar (Gao & Li, 1993), Meyer (Mak, 1995) and biorthogonal (Daubechies, 1992).

The best-known continuous wavelet is Morlet, which also allows the analysis of the phase and the signal module when it is complex (Farge, 1992). The Mexican hat wavelet (Davis et al., 1994; Farge et al., 1996; Chen et al., 1997) is also mentioned in the literature; however, it is generally operated without a complex part. In the present study, we will use Morlet wavelet function and, therefore, it deserves greater attention.

The Morlet function is a complex wavelet that provides a wealth of information about the signal, such as the module and the phase (Farge, 1992; Weng & Lau, 1994; Lau & Weng, 1995). This function has the following equation:

$$\psi(t) = e^{iK_{\psi}t} e^{-(|t|^2/2)} \quad (6)$$

Figure 4 shows the graphs of this function regarding its real and imaginary parts for  $K_{\psi} = 5$ .

With the choice of Morlet WT and the measurements of 600-second temporal series for obtaining the power wavelet spectrum, temperature, and global wavelet spectrum, we obtained results within 95% confidence. The support used was Torrence & Compo (1998) WT modified routines.

### Quadrant Analysis

Antonia (1981), Raupach et al. (1996), Katul et al. (1997), Pope (2000), and Foken et al. (2012) suggest that quadrant analysis can be used to study turbulent fluxes in events associated with vortices ejections or intrusions characterized by coherent structures. The state of the art of this method described by Bolzan et al. (1998) allows correlating two variables through a Cartesian system, i.e., a graph where the abscissa axis is associated with the horizontal component of the wind ( $x = u$ ) and the ordinate axis is associated with the vertical component of the wind ( $y = w$ ), or yet  $x = T$  and  $y = w$  (where  $u$  is the turbulent fluctuation of wind velocity along the flux direction;  $w$  is the fluctuation of vertical velocity; and  $T$  is the temperature fluctuation) according to the goal of the study. Caramori et al. (1994), Bolzan et al. (1998), and Prasad et al. (1998) affirm that the quadrants have better definitions when “upwards” excess or “downwards” excess of a studied flux, or even “upwards” and “downwards” deficit are identified, as shown in Figure 5.

Based on studies conducted by Bolzan et al. (2002), we analysed the “aggregates”. The first quadrant analysis mode showed the dominant quadrants for heat and *momentum* fluxes, and how they behave at different height levels under different atmospheric stability conditions (Fig. 6). In the second mode, we performed simple rotation analysis of the averages of aggregates to establish reliability of fluxes ejections and intrusions.

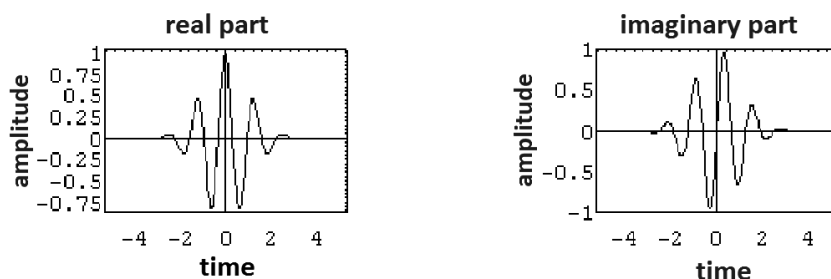


**Figure 4** – Function corresponds to the real part (left); imaginary part of Morlet wavelet (right) considering  $K_{\Psi} = 5$ . (Source: Bolzan, 2000).

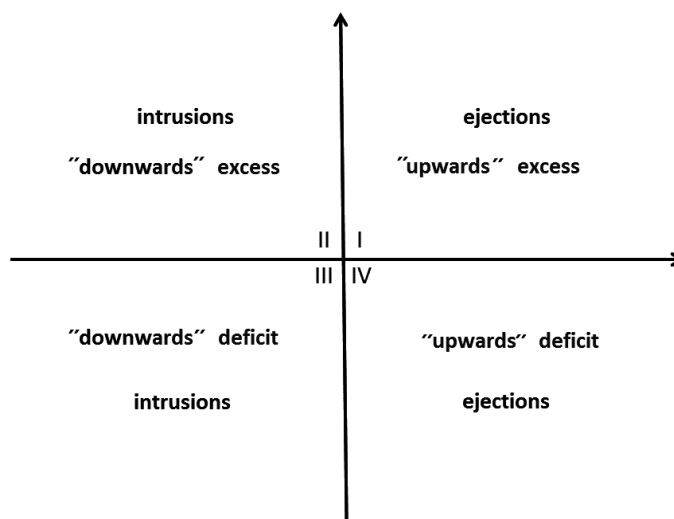


**Figure 5** – Definition of ejections and intrusions for heat flux (unstable conditions) and *momentum* ( $x = w$  and  $y = u$ , in general). Events in quadrants II and IV define intrusions and ejections for the *momentum* flux, whereas quadrants III and I define intrusions and ejections for heat flux ( $x = w$  and  $y = T$ , in general) under unstable conditions.

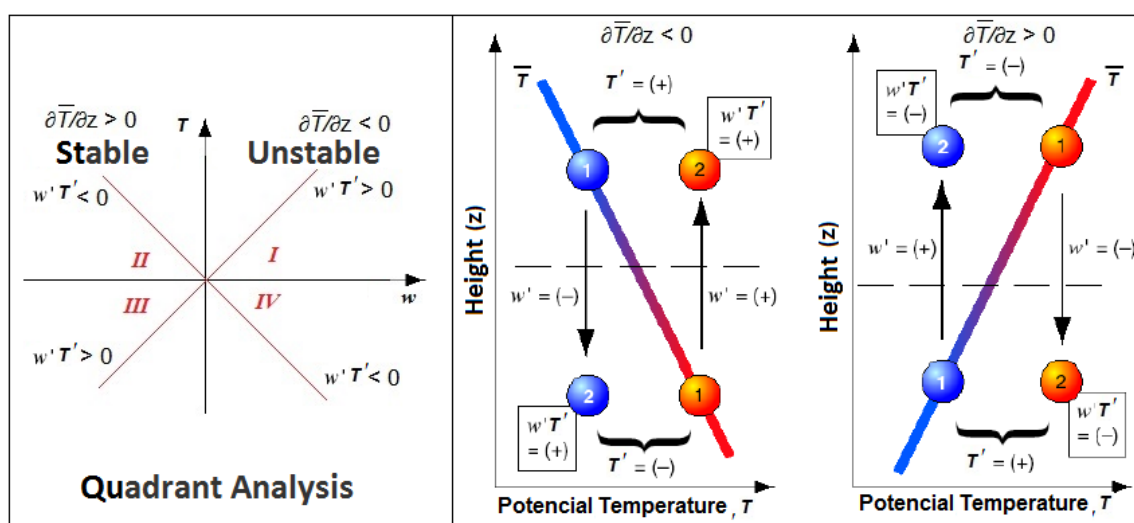


**Figure 6** – “Lapse Rate” and quadrant analysis of sensible heat flux. (Adapted from Stull, 2000).

## RESULTS AND DISCUSSION

### Wind Profile and Inflection Point

We will describe the scenario using Figure 7 which provides information of the Julian day 58, 2012, 02:00 LT, when winds associated with a velocity of up to 15 km/h distort the shape of the forest crown cover opening temporary gaps in the Amazon forest at ATTO, Uatumã SDR and inducing wave movement over and within the forest canopy. This effect reflects the dynamics of the canopy, especially over the rough sub-layer. Generally, it has a typical behaviour of the location regarding the inflection point of the profile of the vertical wind velocity captured by ten ultrasonic anemometers (2D and 3D). For this profile, we forced a polynomial adjustment using least squares procedures, which showed an S-shaped profile. These important characteristics of turbulence including the dynamic effect of instant change caused by shear stress – i.e., rapid change in the wind direction and velocity – indicates an adjacent adverse pressure gradient at these points.

However, Figure 8 shows that the inflection point of the vertical profile of wind velocity was between 50 and 62 m at 10:00 LT, demonstrating that the thermal forcing (heating of the forest crown cover) overlaps the mechanic forcing of the wind shear. As the thermal forcing increases, the inflection point rises at greater heights.

The box-plot diagram in Figure 7 shows little variation between averages and medians of the different heights sampled, indicating that the dispersion was stable, as well as the asymmetry (skewness) of the observed data. Outliers values were determined in the upper ends and below the crown denoting low correlation, which is possibly attributed to strong *momentum* absorption by the canopy and branches. There was also a downwards transfer of movement amount which reduced turbulence. Figure 8 illustrates the variations of different medians and outliers in upper ends at higher levels, suggesting that convection begins to predominate over the wind shear.

Figures 7 and 8 illustrate the loss of *momentum* through the transfer of turbulence in the surface boundary layer through the vegetation branches. This *momentum* loss is proportional to the local mean square velocity, which is a similar condition to that of the definition of drag coefficient for the rough surface and, consequently, to the formation of roll-type coherent structures observed through the vertical profile of wind velocity at certain heights.

Figure 9 shows the quadrant analysis of relative contribution of sensible heat flux at the height of 78 m on Julian day 58, 2012, 1000 LT, following the methodology of Caramori et al. (1994) and Bolzan et al. (1998). This figure shows strong rise of sensible heat flux transport between quadrants 1 and 3 (ejection and intrusion)

) with unstable condition at this height. Under instability, the  $T$  and  $w$  fluctuations have the same sign and generate sensible heat fluxes in the upwards direction (from the crown cover to the atmosphere). As it should be expected, there is clear influence of the atmospheric condition for the sensible heat flux on the configuration of aggregates forms. This can also be understood from the analysis of the atmospheric conditions (day/night) suggested by Stull (1988) regarding the observation of the potential temperature gradient (lapse rate) given by the convective effect (Fig. 6).

Figure 9 validates Figures 7 and 8 through the obtainment of geostationary signals at the frequency of 10 Hz from data obtained by a rapid response instrument (Solent). The graphs of Figure 10 shows that the temperature time series at the height of 78 m, on Julian day 28, 2012, 10:00 LT had significant amplitude growth from 200 s and remained until the end of the observation at 600 s. In addition, it shows ramp-shaped structures, denoting the formation of coherent structures. The wavelet power spectrum exhibited higher energy intensity peaks ranging from 200 to 450 s within the confidence cone, which inserts the 4-6 s period interval, showing a resonance in the responses of the different graphs presented.

The presence of the so-called coherent structures in turbulent flux over a rough surface were observed by the construction of vertical profiles of wind velocity (Figs. 7 and 8). These profiles showed the known inflection point, assuming that the variation of the height at the inflection point can show the timescale (Julian day 58, 02:00 and 10:00 LT) of coherent structures occurring in the thermal field, a phenomenon extremely related to turbulent fluxes of sensible heat.

The results showed an S-shaped curve; however, the uncertainties hamper a single model of vertical profile of wind velocity. In the box-plot attached in Figures 7 and 8, the spacing between the different parts of the diagram help indicate the degree of dispersion (spread) and asymmetry (skewness) of the data, whereas the outliers indicate the low correlation in the *momentum* transfer due to the turbulence, thus hindering the interpretation of the results. However, its importance lies in the universality of the constants involved. There is also a lack of a general theory valid for all types of rough surfaces.

Quadrant analysis was used to determine the formation of coherent structures. We related the component of the wind velocity in the vertical direction ( $w$ ) and temperature ( $T$ ) and assessed the data obtained by rapid response instruments which were sampled simultaneously with measurements performed at ten different heights using the covariance method (Eddy Covariance) (Fig. 9).

The dominant aggregate concentration quadrants were mainly located in quadrants 1 and 3, i.e., between ejection and intrusion, both for heat fluxes and the *momentum*. In addition, their distri-



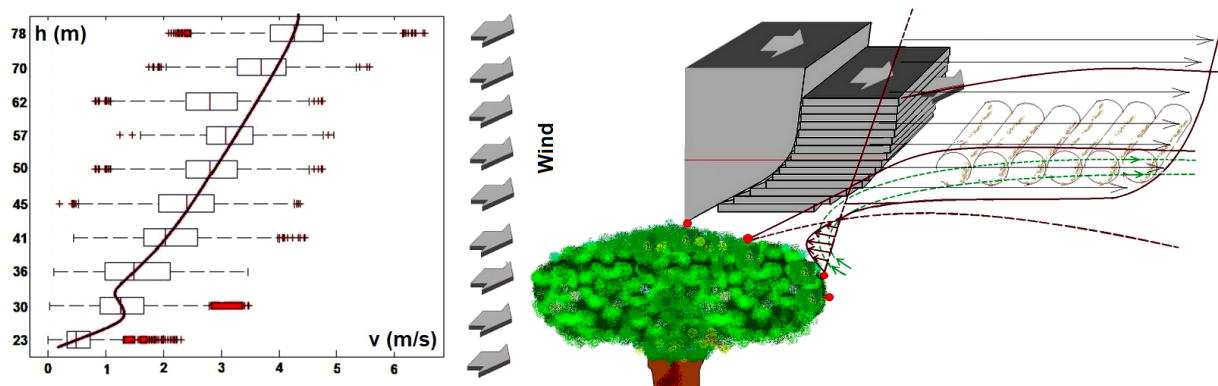


**Figure 7** – Box-plot diagrams, with the inflection point of the wind velocity, with an adjusted polynomial curve. On the right is a pictorial diagram of the inflection point of the wind shear with the formation of coherent “roll” structures above the tree canopy in the study area at 02 LT, for the 58th Julian day of 2012.

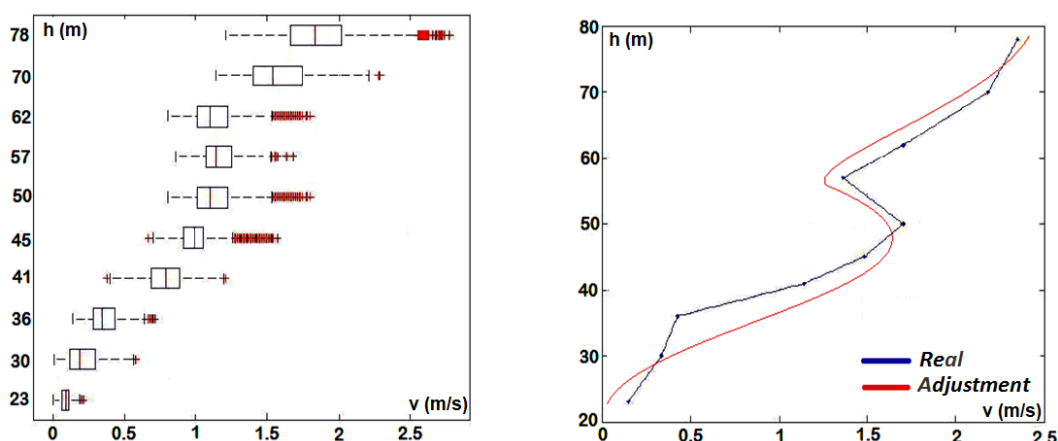


**Figure 8** – Box-plot diagrams, with the inflection point of the wind velocity, with an adjusted polynomial curve. On the right is the setting without the boxes, the inflection is associated with wind shear and thermal forcing on the canopy of the local trees, at 10 LT, for the 58th Julian day of 2012.

butions varied under atmospheric stability conditions, exhibiting a tendency to reflect the existence of coherent structures in the form of “rolls” generated by the instability of the inflection point (Fig. 11). The use of Morlet wavelet transform (Fig. 11) allowed to observe the growth of convective effect from 200 to 350 s caused by the heating of the canopy, a phenomenon with a period of 150 s. It was also possible to observe the occurrence of considerably intermittent periods that were shorter than 16 s, i.e., periods that occur during timescales without any periodicity.

## CONCLUSIONS

The results from this work, that had the result of investigating characteristics of turbulence in a forest in the Central Amazônica, indicate that for the study period from February to September 2012, at the ATTO-CLAIRE site, the most important results are:

1. The presence of coherent structures (ECs) in turbulent

flux above a rough surface of the forest canopy in the ATTO-CLAIRE experiment (IOP-1/2012), in a *terra firme* forest (Central Amazônica), were detected after the inflexion point of the average wind velocity, using box-plot diagrams, quadrant analyses, and wavelet transformation in the wet and dry seasons.

2. The results from the ATTO-CLAIRE experiment (IOP-1/2012), are in agreement with those described by Wallace (1972), Hussain (1986), Katul et al. (1997), and Bolzan et al. (1998), according to which, when there are variations in stability conditions, there is an influence of time on the duration of coherent structures. Therefore, this study demonstrated a robustness in the identification of coherent structures denominated as “rolls” for the studied flux, as was also demonstrated by Raupach & Thom (1981), Raupach et al. (1996), Bolzan (2000) and Bolzan & Vieira (2006).

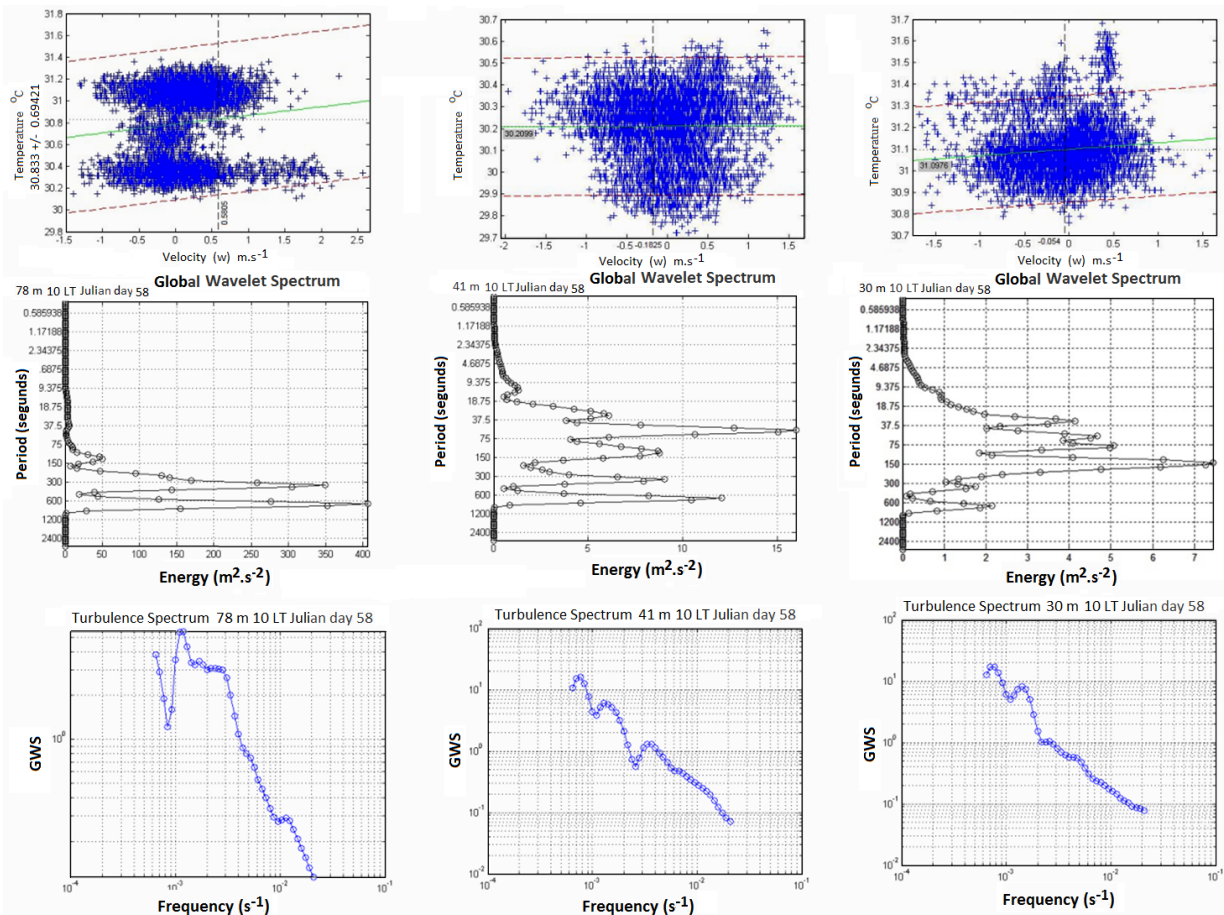


**Figure 9** – Quadrant analysis panels, global wavelet spectrum, and power spectrum ( $w'$  and  $T'$ ), Julian day 58, 2012, 1000 LT. The columns are arranged from left to right at heights of 78, 41, and 30 m. There is a tendency for ejection and intrusion between the quadrants in the three top figures. The global wavelet spectrum and the energy spectrum show the characteristics of turbulence above and within the canopy.

## ACKNOWLEDGEMENTS

The authors are thankful to the National Institute of Amazonia Research (INPA/MCTI), the State University of Amazonas (UEA), and the Max Planck Institute for Biogeochemistry through the Brazil-Germany agreement at Amazon Tall Tower Observatory (ATTO), during the field research conducted in the present study. We are also thankful to Torrence and Compo for the use of their routines of wavelet transform at <http://atoc.colorado.edu/research/wavelets>.

## REFERENCES

- AMARAL IL, MATOS FDA & LIMA J. 2000. Composição Florística e Parâmetros Estruturais de um hectare de Floresta Densa de Terra Firme no Rio Uatumã, Amazônia, Brasil. *Acta Amazônica*, 30(3): 377–392.
- ANDRAE MO, ACEVEDO OC, ARAÚJO A, ARTAXO P, BARBOSA CGG, BARBOSA HMJ, BRITO J, CARBONE S, CHI X, CINTRA BBL, DA SILVA NF, DIAS NL, DIAS-JÚNIOR CQ, DITAS F, DITZ R, GODOI AFL, GODOI RH, HEIMANN M, HOFFMANN T, KESSELMEIER J, KÖNEMANN T, KRÜGER ML, LAVRIC JV, MANZI AO, LOPES AP, MARTINS DL, MIKHAILOV EF, MORAN-ZULOAGA D, NELSON BW, NÖLSCHER AC, SANTOS NOGUEIRA D, PIEDADE MTF, PÖHLKER C, PÖSCHL U, QUESADA CA, RIZZO LV, RO C.-U, RUCKTESCHLER N, SÁ LDA, OLIVEIRA SÁ M, SALES CB, SANTOS RMN, SATURNO J, SCHÖNGART J, SÖRGEL M, SOUZA CM, SOUZA RAF, SU H, TARGHETTA N, TÓTA J, TREBS I, TRUMBORÉ S, VAN EIJCK A, WALTER D, WANG Z, WEBER B, WILLIAMS J, WINDERLICH J, WITTMANN F, WOLFF S & YÁÑEZ-SERRANO AM. 2015. The Amazon Tall Tower Observatory (ATTO): overview of pilot measurements on ecosystem ecology, meteorology, trace gases, and aerosols. *Atmos. Chem. Phys.*, 15: 10723–10776.
- ANTONIA R. 1981. Conditional Sampling in Turbulence Measurement. *Ann. Rev. Fluid Mech.*, 13: 131–156.
- BALDOCCHI DD & MEYERS TP. 1988. Turbulence Structure in a Deciduous Forest. *Boundary-Layer Meteorology*, 43: 345–364.

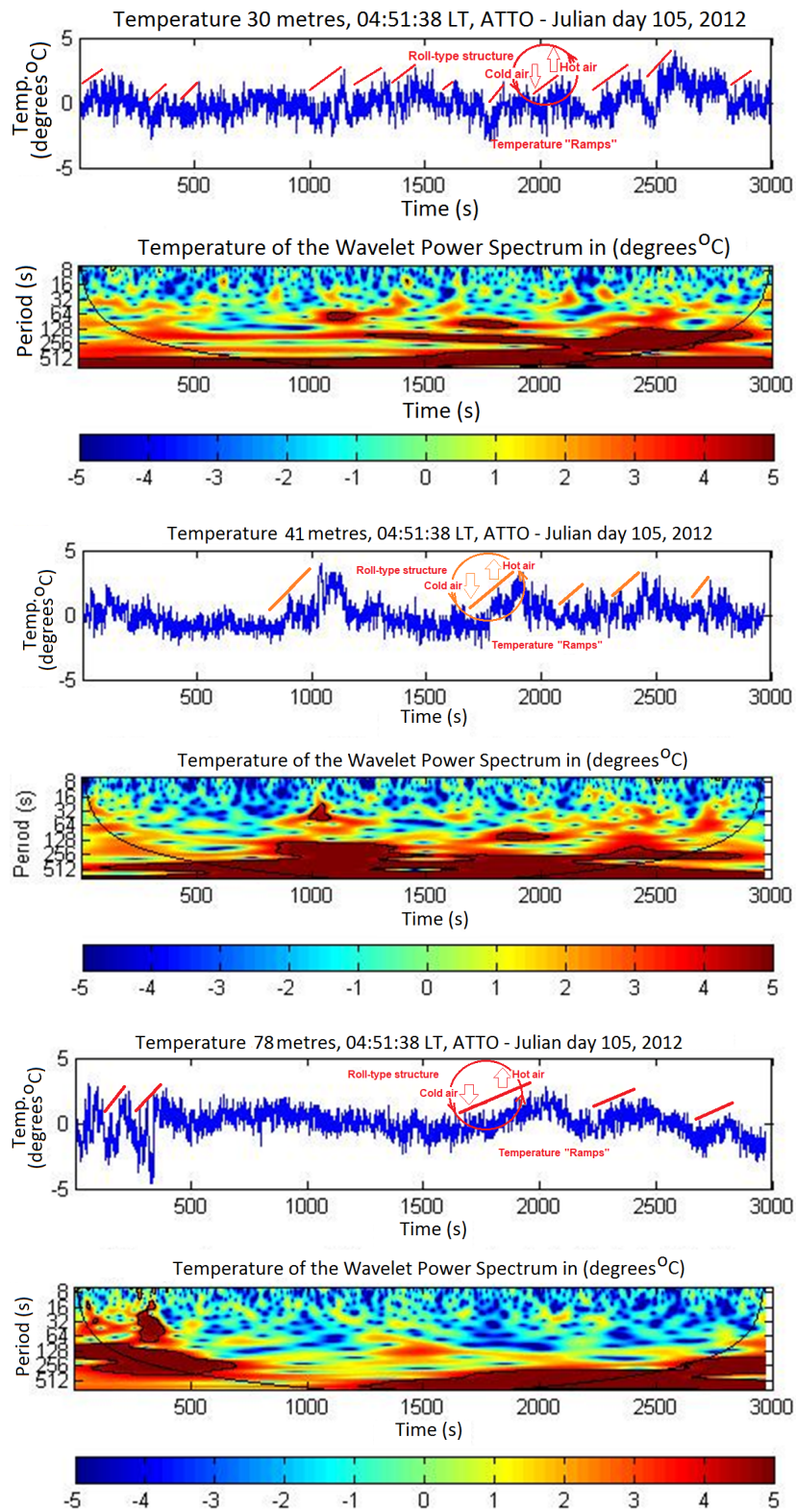


**Figure 10** – Wavelet transform panels showing the form of coherent structures (type: ramp or roll) at three height levels (30, 41, and 78 m), i.e., at 09:56:27 (LT) above and within the forest canopy at ATTO, for the 105th Julian day of 2012. (Source: UEA-INPA-MAX PLANCK, 2012).

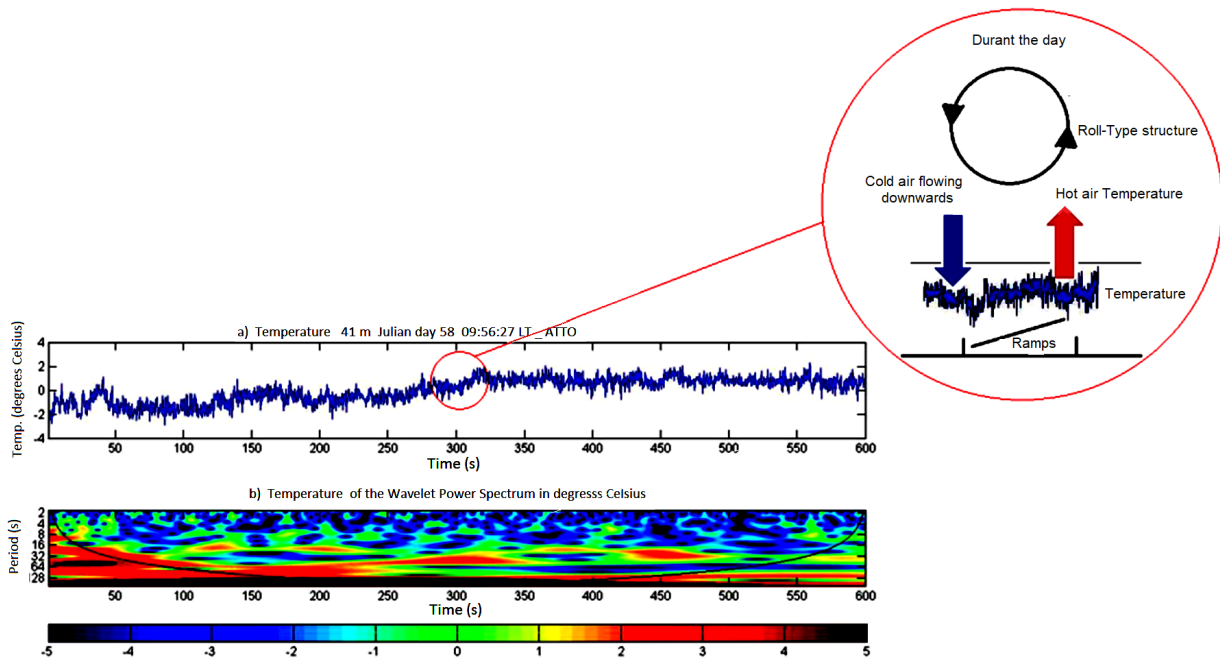


**Figure 11** – Existence of roll- and ramp-type coherent structures due to the instability of the inflection point of the vertical profile of the wind over the canopy (41 m) on Julian day 58, 2012, 09:56:27 LT. (Source: UEA-INPA-MAX PLANCK, 2012).

BOLZAN MJA. 2000. Estudo da influência das Estruturas Coerentes e da rugosidade na estimativa de fluxos turbulentos sobre o Pantanal. São José dos Campos. Dissertation, Master's degree in Meteorology – Instituto Nacional de Pesquisas Espaciais (INPE-7500-TDI/715). São Paulo, Brazil. 71 pp.

BOLZAN MJA & VIEIRA PC. 2006. Wavelet Analysis of the Wind Velocity and Temperature Variability in the Amazon Forest. *Brazilian Journal of Physics*, 36(4A): 1217–1222.

BOLZAN MJA, PRASAD GSSD, SÁ LDA, ALVALÁ RCS, SOUZA A & KASSARE E. 1998. Análise de quadrante aplicada a flutuações turbulentas acima do Pantanal (estação seca). In: II Método de Caramori. X Congresso Brasileiro de Meteorologia, Brasília, Brazil, 26-30 October.

BOLZAN MJA, RAMOS FM, SÁ LDA, NETO CR & ROSA RR. 2002. Analysis of fine-scale canopy turbulence within and above an Amazon Forest using Tsallis' generalized thermostatics. *Journal of Geophysical Research*, 107(D20): LBA 30-1–LBA 30-7.

CAMPANHARO ASLO, RAMOS FM & MACAU EEN. 2005. Análise de sinais turbulentos na copa da floresta amazônica: em busca de caos e estruturas coerentes. In: WORCAP 2005. Proceedings, INPE, São José dos Campos, Brazil.

CARAMORI P, SCHUEPP P, DESJARDINS R & MacPHERSON I. 1994. Structural Analysis of Airborne Flux Estimates over a Region. *Journal of Climate*. American Meteorological Society, 7: 627–640.

CHEN W, NOVAK MD, BLACK TA & LEE X. 1997. Coherent eddies and temperature structure functions for three contrasting surfaces. Part I:

Ramp model with finite microfront time. *Boundary-Layer Meteorology*, 84(1): 99–123.

DAVIS A, MARSHAK A, WISCOMBE W & CAHALAN R. 1994. Multifractal characterizations of non-stationary and intermittency in geophysical fields: Observed, retrieved, or simulated. *Journal of Geophysical Research*, 99(D4): 8055–8072.

DENNIS DJC. 2015. Coherent structures in wall-bounded turbulence. *Anais da Academia Brasileira de Ciências (Annals of the Brazilian Academy of Sciences)*, 87(2): 1161–1193.

DIAS JR CQ, SÁ LDA, MARQUES FILHO EP, MANZI AO, TREBS I & WINDERLICH J. 2013. Variabilidade Vertical de Estruturas Coerentes na Camada Limite Convectiva da Amazônia. *Revista do Centro do Ciências Naturais e Exatas – UFSM. Revista Ciência e Natura*, ISSN: 2179-460X. Santa Maria, Brazil, ed. esp.: 131–133.

FARGE M. 1992. The Wavelet Transform and its applications to turbulence. *Annual Review of Fluid Mechanics*, 24: 395–457.

FARGE M, KEVLAHANN, PERRIER V & GOIRAND E. 1996. Wavelets and turbulence. In: Proceedings of the IEEE, 84(4): 639–669.

FOKEN T. 2008. *Micrometeorology*. Springer-Verlag Berlin Heidelberg, 320 pp.

FOKEN T, MEIXNER FX, FALGE E, ZETZSCH C, SERAFIMOVICH A, BARGSTEN A, BEHRENDT T, BIERMANN T, BREUNINGER C, DIX S, GERKEN T, HUNNER M, LEHMANN-PAPE L, HENS K, JOCHER G, KESSELMEIER J, LÜERS J, MAYER J-C, MORAVEK A, PLAKE D,

- RIEDERER M, RÜTZ F, SCHEIBE M, SIEBICKE L, SÖRGEL M, STAUDT K, TREBS I, TSOKANKUNKA, WELLING M, WOLFF V & ZHU Z. 2012. Coupling processes and exchange of energy and reactive and non-reactive trace gases at a forest site – results of the EGER experiment. *Atmos. Chem. Phys.*, 12: 1923–1950.
- GAO W & LI BL. 1993. Wavelet analysis of coherent structures at the atmosphere-forest interface. *Journal of Applied Meteorology*, 32(11): 1717–1725, Nov.
- GASQUET C & WITOMSKI P. 1990. *Analyse de Fourier et applications*. Masson, Paris, 354 pp.
- HUSSAIN AKMF. 1983. Coherent structures – reality and myth. *Physics of Fluids*, 26: 35 pp. doi:10.1063/1.864048.
- KAIMAL JC & FINNIGAN JJ. 1994. *Atmospheric Boundary Layer Flows (Their structure and measurement)*. NY, Oxford, Oxford University Press. 304 pp.
- KATUL G, KUHN G, SCHIEDGE J & CHENG-I HSIEH. 1997. The ejection-sweep character of scalar fluxes in the unstable surface layer. *Boundary-Layer Meteorology*, 83(1): 1–26.
- KRUIJT B, MALHI Y, LLOYD J, NORBRE AD, MIRANDA AC, PEREIRA MGP, CULF A & GRACE J. 2000. Turbulence statistics above and within two Amazon rain forest canopies. *Boundary-Layer Meteorology*, 94: 297–331.
- LAU K-M & WENG H. 1995. Climate signal detection using Wavelet Transform: How to make a time series sing. *Bulletin of the American Meteorological Society*, 76(12): 2391–2402.
- LIMA NS, TÓTA J, BOLZAN MJA, VALE R & SANTANA R. 2013. Característica Aerodinâmica da Turbulência sobre e dentro do Dossel de uma Floresta de Terra Firme na Amazônia Central. *Revista do Centro de Ciências Naturais e Exatas – UFSM. Revista Ciência e Natura*, ISSN: 2179-460X. Santa Maria, Brazil, ed. esp.: 375–379.
- LLOYD CR, SHUTTLEWORTH WJ, GASH JHC & TURNER M. 1984. A Microprocessor System for Eddy Correlation. *Agricultural and Forest Meteorology*, 33: 63–76.
- MAK M. 1995. Orthogonal wavelet analysis: Interannual variability in the sea surface temperature. *Bulletin of American Meteorological Society*, 76(11): 2179–2186.
- MEYER Y. 1990. *Ondelettes – Ondelettes et opérateurs*. I. Hermann, Paris, 215 pp.
- OLIVEIRA LS. 2008. Refinamento da representação de raízes no modelo de biosfera SiB2 em área de floresta na Amazônia. Dissertation, Master's degree in Environmental Sciences – Graduate Programme in Environmental Sciences, Geosciences Institute, Universidade Federal do Pará, Museu Emílio Goeldi and EMBRAPA, Belém, Brazil. 66 pp.
- POPE SB. 2000. *Turbulent Flows*. Cambridge University Press, 312 pp. (digital version).
- PRASAD GSSD, SÁ LDA, BOLZAN MJA & ALVALÁ RCS. 1998. Análise de quadrante aplicada a flutuações turbulentas acima do Pantanal (estação seca). I Método de Katul, variabilidade em função da estabilidade atmosférica. In: X Brazilian Conference in Meteorology, Brasília, Brazil, p. 26–30.
- RANKIN-DE-MÉRONA J, PRANCE GT, HUTCHINGS RW, SILVA MF da, RODRIGUES WA & VENLING ME. 1992. Preliminary results of a large-scale tree inventory of upland rain forest in the Central Amazon. *Acta Amazonica*, 22(4): 485–492.
- RAUPACH MR & THOM AS. 1981. Turbulence in and above plant canopies. *Ann. Rev. Fluid Mechanics*, 13: 97–129.
- RAUPACH MR, FINNIGAN JJ & BRUNET Y. 1996. Coherent eddies and turbulence in vegetation canopies: The mixing-layer analogy. *Boundary-Layer Meteorology*, 78(3-4): 351–382.
- STULL RB. 1988. *An Introduction to Boundary Layer Meteorology (Atmospheric Science Library)*, Kluwer Academic Publishers, The Netherlands, 666 pp.
- STULL RB. 2000. *Meteorology for Scientists and Engineers. A Technical Companion Book to C. Donald Ahrens' Meteorology Today*. 2nd ed., 523 pp.
- TELLO JCR. 1995. Aspectos fitossociológicos das comunidades vegetais de uma topossequência da Reserva Florestal Ducke do INPA. Doctorate Thesis, INPA/FUA, Manaus, AM, Brazil. 335 pp.
- TENNEKES H & LUMLEY JL. 1972. *A First Course in Turbulence*. The MIT Press; Cambridge, Massachusetts, and London, England, 310 pp.
- TORRENCE C & COMPO GP. 1998. A Practical Guide to Wavelet Analysis. *Bulletin of the American Meteorological Society*, 79(1): 61–79.
- VALENCIA R, BALSLEV H & MIÑO CGPY. 1994. High tree alpha-diversity in Amazonian Ecuador. *Biodiversity and Conservation*, 3: 21–28.
- WALLACE JM & HOBBS PV. 2006. *Atmospheric Science: An Introductory Survey*. In: DMOWSKA R, HARTMANN D & ROSSBY HT (Eds.). *International Geophysics Series*, Vol. 92, 2nd ed., 505 pp.
- [www.wwf.org/what\\_we\\_do/where\\_we\\_work/amazon/about\\_the\\_amazon/ecosystems\\_amazon/rivers/](http://www.wwf.org/what_we_do/where_we_work/amazon/about_the_amazon/ecosystems_amazon/rivers/) WWF, U.S. Geological Survey, ICTA, TNC, University of Kassel (retrieved: September 2012).

Recebido em 11 julho, 2017 / Aceito em 8 dezembro, 2017  
 Received on July 11, 2017 / Accepted on December 8, 2017